Two-color Transient Grating Spectroscopy of a Two-level System

Kyungwon Kwak, Minhaeng Cho,* Graham R. Fleming,*,† Ritesh Agarwal,† and Bradley S. Prall†

Department of Chemistry and Center for Multidimensional Spectroscopy, Korea University, Seoul 136-701, Korea
†Department of Chemistry, University of California, Berkeley and Physical Biosciences Division, Lawrence Berkeley National Laboratory, Berkeley, California 94720, U.S.A.
Received April 14, 2003

A theoretical description and experimental demonstration of homodyne-detected two-color transient grating (2-C TG) signal are presented. By treating the coupled bath degrees of freedom as a collection of harmonic oscillators and using a short-time expansion method, approximated nonlinear response functions were obtained. An analytic expression for the two-color transient grating signal was obtained by carrying out relevant Gaussian integrals. The initial rising and decaying parts of the 2-C TG signal is shown to be critically dependent on the ultrafast inertial component of the solvation correlation function. The experimental results confirm the predictions of the theoretical model.

Key Words : Transient grating, Solvation, Spectroscopy

Introduction

Four-wave-mixing transient grating spectroscopy[1-3] can be viewed as a one-dimensional vibrational spectroscopy that is capable of probing vibrational dynamics and chromophore-solvent relaxation processes on both the ground and excited states.[4-6] By injecting two simultaneously propagating pulses in time with different wavevectors, vibrational coherence states are created on the ground as well as excited states. Since the pulse widths are sufficiently short to excite vibrational modes that are coupled to an electronic transition of the chromophore, the electronic dephasing process induced by the fluctuating chromophore-solvent interaction energy can be studied with this transient grating spectroscopy. In the present paper, we will consider two-color transient grating spectroscopy (2C-TG), where the pump and the probe frequencies are different from each other.[7,8] In this case, the initial wavepacket or doorway state, created by the interactions with the pump pulses is located at a different region of phase space than that of the window specified by the width and frequency of the probe pulse. On the other hand, in the case of conventional 1-C TG, the phase space region of the initial wavepacket is identical with the window state.[9] Therefore, 1-C TG measures how rapidly the initial wavepacket moves away from the initial phase space region. Consequently, the 1-C TG signal decays monotonically. In contrast, due to the difference between the doorway phase space and the window phase space, the 2-C TG signal can rise initially and reach a maximum value at the time when the propagating wavepacket passes through the window phase space. Due to this additional experimental controllability of the 2-C TG, it becomes possible to explore a much wider region of the phase space stet spanned by the coupled bath degrees of freedom. A theoretical description of the 2-C TG signal and numerical calculations for a few model systems will be presented in sections II and III, respectively, while in section IV experimental results are presented for two systems.

*Co-Corresponding authors. Minhaeng Cho (E-mail: mcho@korea.ac.kr); Graham R. Fleming (E-mail: grfleming@lbl.gov)

Theoretical

We will consider a two electronic level system interacting with external electric fields. Two pulses propagating with wavevectors of $\mathbf{k}_1$ and $\mathbf{k}_2$ are used to create particles and holes on the excited and ground states, respectively. Then the third pulse which is delayed in time, is injected and the scattered signal field in the direction of $-\mathbf{k}_1 + \mathbf{k}_2 + \mathbf{k}_3$ is detected by employing homodyne or heterodyne methods. The frequencies of the pump (the first two pulses) fields and the probe field will be denoted as ω_{pu} and ω_{pr}, respectively.

Then, the third-order polarization associated with the TG signal is given as[10]

$$\begin{aligned} P^{(3)}(\mathbf{k}_s,t) = \left(\frac{i}{\hbar}\right)^3 \int_0^\infty dt_1 \int_0^\infty dt_2 \int_0^\infty dt_3 [R_1 + R_4] \\ \times E_3(t-t_3) E_1^*(t+\tau-t_3-t_2) \\ \times E_2(t+\tau-t_3-t_2-t_1) \exp(i\omega_{pr}t_3 + i\omega_{pu}t_1) \\ + \int_0^\infty dt_1 \int_0^\infty dt_2 \int_0^\infty dt_3 [R_2 + R_3] E_3(t-t_3) E_2(t+\tau-t_3-t_2) \\ \times E_1^*(t+\tau-t_3-t_2-t_1) \exp(i\omega_{pr}t_3 - i\omega_{pu}t_1) . \end{aligned} \quad (1)$$

Here, the pulse envelopes are denoted by E_j (j = 1-3). The homodyne-detected TG signal is given by the integrated intensity of the TG signal field that is linearly proportional to the square of the above third-order polarization within the slowly-varying-amplitude approximation, *i.e.*,

$$S(\omega_{pu}, \omega_{pr}; \tau) = \int_{-\infty}^{\infty} dt \left| P^{(3)}(\mathbf{k}_s, t) \right|^2 \quad (2)$$

Now, let's change the integration variable t to $t + t_3$ and

introduce a new integration variable $t' = t + \tau - t_2$. Then, we have

$$P^{(3)}(\mathbf{k}_s,t) = \left(\frac{i}{\hbar}\right)^3 E_3(t)\int_0^\infty dt_1 \int_{-\infty}^{\infty} dt' \int_0^\infty dt_3 E_1^*(t')E_2(t'-t_1)$$
$$\times \{(R_1+R_4)\exp[i\omega_{pr}t_3 + i\omega_{pu}t_1]$$
$$+ (R_2+R_3)\exp[i\omega_{pr}t_3 - i\omega_{pu}t_1]\} \quad (3)$$

where $R(t_1,t_2,t_3) \to R(t_1,t+\tau-t',t_3)$. In order to obtain Eq. (3), we assumed that the delay time τ is sufficiently larger than the pulse width such that the upper limit of the integration over t' can be replaced with ∞.

A. Approximate nonlinear response function. The general nonlinear response function of a two-level system was presented before and is given by a sum of the following four components and their complex conjugates,[9]

$$R_1(t_3,t_2,t_1) = \exp(-i\omega_{eg}t_1 - i\omega_{eg}t_3)$$
$$\times \exp\{-g^*(t_3) - g(t_1) - f_-(t_3,t_2,t_1)\}$$
$$R_2(t_3,t_2,t_1) = \exp(i\omega_{eg}t_1 - i\omega_{eg}t_3)$$
$$\times \exp\{-g^*(t_3) + -g^*(t_1) + f_+^*(t_3,t_2,t_1)\}$$
$$R_3(t_3,t_2,t_1) = \exp(i\omega_{eg}t_1 - i\omega_{eg}t_3)$$
$$\times \exp\{-g(t_3) + -g^*(t_1) + f_-^*(t_3,t_2,t_1)\}$$
$$R_4(t_3,t_2,t_1) = \exp(-i\omega_{eg}t_1 - i\omega_{eg}t_3)$$
$$\times \exp\{-g(t_3) - g(t_1) - f_-(t_3,t_2,t_1)\} \quad (4)$$

where the two auxiliary functions are defined as

$$f_+(t_3,t_2,t_1) = g^*(t_2) - g^*(t_2+t_3) - g(t_1+t_2)$$
$$+ g(t_1+t_2+t_3)$$
$$f_-(t_3,t_2,t_1) = g(t_2) - g(t_2+t_3) - g(t_1+t_2)$$
$$+ g(t_1+t_2+t_3) \quad (5)$$

Here, the line broadening function, $g(t)$, is[11]

$$g(t) = -i\frac{\lambda}{\hbar}t + \int_0^\infty d\omega\rho(\omega)\coth\left[\frac{\hbar\omega\beta}{2}\right](1-\cos\omega t)$$
$$+ i\int_0^\infty d\omega\rho(\omega)\sin\omega t \quad (6)$$

The spectral density representing system-bath coupling strengths and frequency distribution of the coupled bath modes was denoted as $\rho(\omega)$.

Noting that the electronic coherence relaxation time during the t_3-period is typically very short, one can use the following truncated Taylor expansion forms,

$$g(t_2+t_3) = g(t_2) + \left(\frac{\partial g(t_2+t_3)}{\partial t_3}\right)_{t_3=0} t_3 + \cdots$$
$$g(t_1+t_2+t_3) = g(t_1+t_2) + \left(\frac{\partial g(t_1+t_2+t_3)}{\partial t_3}\right)_{t_3=0} t_3 + \cdots. \quad (7)$$

where

$$\left(\frac{\partial g(T+t_3)}{\partial t_3}\right)_{t_3=0} = i\left(\int_0^\infty d\omega\rho(\omega)\,\omega\cos\omega T - \frac{\lambda}{\hbar}\right)$$
$$+ \int_0^\infty d\omega\rho(\omega)\coth\left[\frac{\hbar\omega\beta}{2}\right]\omega\sin\omega T = iQ(T) + H(T) \quad (8)$$

With this short time expansion approximation, the two auxiliary functions, f_+ and f_-, can be approximately written as

$$f_-(t_3,t_2,t_1) = (iQ(t_2) - H(t_2))t_3$$
$$+ (iQ(t_1+t_2) + H(t_1+t_2))t_3$$
$$f_-(t_3,t_2,t_1) = (-iQ(t_2) - H(t_2))t_3$$
$$+ (iQ(t_1+t_2) + H(t_1+t_2))t_3 \quad (9)$$

where $t_2 = t + \tau - t'$.

We further assume that $t_2 = t + \tau - t' \cong \tau$ and $t_1 + t_2 = t + \tau - t' + t_1 \cong \tau$ to find

$$f_- \cong 2iQ(\tau)t_3$$
$$f_- \cong 0. \quad (10)$$

Also, using a short-time approximation for $g(t)$ with respect to t_1 and t_3, we have

$$g(t_1) = g^*(t_1) = \frac{1}{2}\hat{\Omega^2}\hat{t_1^2} \text{ and } g(t) = g^*(t_3) = \frac{1}{2}\hat{\Omega^2}\hat{t_3^2} \quad (12)$$

where the mean square fluctuation amplitude of the electronic transition frequency is defined as

$$\hat{\Omega^2} \equiv \int d\omega\rho(\omega)\omega^2\coth\frac{\hbar\omega\beta}{2}. \quad (13)$$

Thus, the four response function components in Eq. (4) can be simplified to

$$R_1 = \exp(-i\omega_{eg}t_1 - i\omega_{eg}t_3)$$
$$\times \exp\left\{-\frac{1}{2}\Omega^2t_1^2 - \frac{1}{2}\Omega^2t_3^2 - 2iQ(\tau)t_3\right\}$$
$$R_2 = \exp(i\omega_{eg}t_1 - i\omega_{eg}t_3)$$
$$\times \exp\left\{-\frac{1}{2}\Omega^2t_1^2 - \frac{1}{2}\Omega^2t_3^2 - 2iQ(\tau)t_3\right\}$$
$$R_3 = \exp(i\omega_{eg}t_1 - i\omega_{eg}t_3)\exp\left\{-\frac{1}{2}\Omega^2t_1^2 - \frac{1}{2}\Omega^2t_3^2\right\}$$
$$R_4 = \exp(-i\omega_{eg}t_1 - i\omega_{eg}t_3)\exp\left\{-\frac{1}{2}\Omega^2t_1^2 - \frac{1}{2}\Omega^2t_3^2\right\}. \quad (14)$$

B. 2-C TG polarization. In order to take into account the finite pulse width effect on the 2-C TG signal, the pulse envelope functions are assumed to be identical and of a Gaussian form, *i.e.* as $E(t) = \exp(-t^2/2\Delta^2)$ where the

standard deviation is denoted by Δ. Inserting Eqs. (14) and Gaussian pulse envelope functions into Eq. (3) and calculating the integrals over t_1 and t', we find

$$P^{(3)}(k_s,t) \propto i^3 E_3(t)\exp(-X^2)$$
$$\times\left\{ \exp(-I^2(\tau)) + \frac{2i}{\sqrt{\pi}}F(Y(\tau)) + \exp(-I^2(0)) + \frac{2i}{\sqrt{\pi}}F(Y(0)) \right\} \tag{15}$$

where

$$X \equiv \frac{\omega_{pu} - \omega_{eg}}{\sqrt{2[\Omega^2 + \Delta^{-2}]}}$$
$$Y(\tau) \equiv \frac{\omega_{pr} - \omega_{eg} - 2\{S(\tau) - \lambda/\hbar\}}{\sqrt{2\Omega^2}} \tag{16}$$

In the above equation (15), $S(t)$ is the solvation correlation function that can be expressed in terms of the spectral density as

$$S(t) = \int d\omega\ \omega\rho(\omega)\cos\omega t\,. \tag{17}$$

and the solvation reorganization energy is

$$\lambda = \hbar\int d\omega\ \omega\rho(\omega)\,. \tag{18}$$

The Dawson integral, $F(x)$, in Eq. (15) is defined as[12]

$$F(x) = e^{-x^2}\int_0^x du\ e^{u^2}\,. \tag{19}$$

Eq. (15) constitutes the principal result of the present paper. Because of the τ-dependent terms in Eq. (15), the third-order TG polarization provides information on the spectral diffusion induced by the chromophore-solvent dynamics. Also, it should be noted that the polarization is complex. If one carries out a heterodyne detection experiment, it would be possible to measure the real and imaginary parts of the polarization separately. The real and imaginary parts of the polarization correspond to the transient birefringence and the transient dichroism, respectively.[13]

The homodyne-detected transient grating signal can now be calculated and found to be

$$S_{TG}(\tau) \propto \int_{-\infty}^{\infty} dt\left|P^{(3)}(k_s,t)\right|^2$$
$$\propto \exp(-2X^2)\left\{ [\exp(-Y^2(\tau)) + \exp(-Y^2(0))]^2 \right.$$
$$\left. + \frac{4}{\pi}[F(Y(\tau)) + F(Y(0))]^2 \right\} \tag{20}$$

Numerical Calculation Results

In this section, we will present numerically calculated 1-C and 2-C TG signals for a simple model system. The solvation reorganization energy, λ, will be assumed to be 600 cm^{-9}. In the high-temperature limit, the mean square fluctuation amplitude, Ω^2, of the electronic transition frequency is related to λ by ($\Omega^2 \equiv 2\lambda k_B T/\hbar^2$) where k_B and T are the Boltzmann constant and the temperature, respectively.[14]

We next assume that the solvation correlation function, $S(t)$, consists of two components, *i.e.*, a Gaussian and an exponential component with the form[5]

$$S(t) = \frac{\lambda}{\hbar}\frac{\{\exp(-t^2/\Gamma^2) + 0.5\exp(-2t)\}}{1.5} \tag{21}$$

where the unit of time is the picosecond. The ratio of the Gaussian component to the exponential component is 1 : 0.5. In the following calculations, the Gaussian decay constant Γ will be varied to investigate the Γ-dependence of the 2-C TG signal.

Throughout the present paper, the pump field frequency will be assumed to be in resonance with the absorption band maximum, *i.e.*, $\omega_{pu} = \omega_{eg}$. Although the approximate expression for the TG polarization in Eq. (15) is useful, it should be noted that Eq. (15) cannot be used to describe the case when the pump field frequency deviates from ω_{eg}. A more general theory is currently being developed and will be presented elsewhere. In the present paper, we will focus on the case when only the probe field frequency is tunable and the detuning factor W is defined as

$$W \equiv \omega_{eg} - \omega_{pr}\,. \tag{22}$$

A. One-color TG signal. One-color TG signals are calculated for varying Γ (=100, 200, 300, 400, and 500 fs) and plotted in Figure 1(a). As in the work of Joo *et al.*,[5] the initial decaying part of the 1-C TG signal is found to be dependent on the ultrafast component of $S(t)$. In this case of the 1-C TG, the phase space region of the initially created wavepacket is identical to that of the window so that the signal at time zero is maximum and then decreases as the wavepacket moves away from the phase space region of the window. In Figure 1(b), the two contributions from the transient birefringence and dichroism, when Γ = 100 fs, are separately plotted and the figure shows that the transient dichroic contribution is dominant in this case.

B. Two-color TG signal. We next calculate the two-color TG signal. In order to investigate the detuning-factor-dependence of the 2-C TG signal, by varying W from 0 to 1400 cm^{-1}, a series of downhill (*i.e.*, $\omega_{pu} > \omega_{pr}$) 2-C TG signals are plotted in Figure 2(a). A positive value of W corresponds to a 'downhill' 2-C TG experiment with the third frequency being lower than the first two.

As the detuning factor W increases, the signal exhibits a non-monotonic behavior. For instance, if W = 800 cm^{-1}, the location of the window is, along the solvation coordinate, 800 cm^{-1} away from that of the initially created wavepacket so that it takes a finite time (about 80 fs) for the propagating wavepacket to reach the window region. This means that the detuning factor, W, determines the energy separation

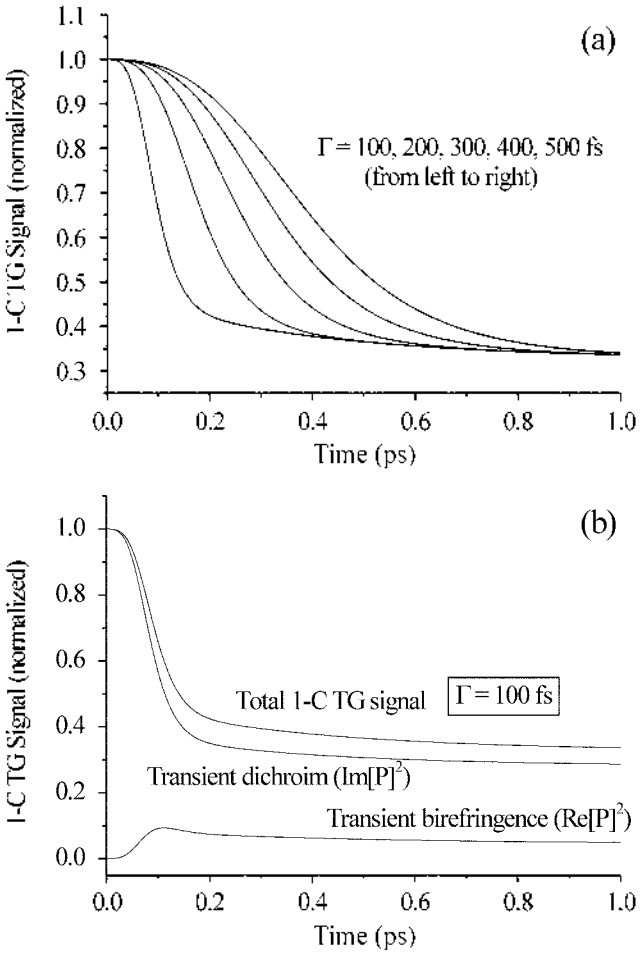

Figure 1. (a) Calculated 1-C TG signals for Γ = 100, 200, 300, 400, and 500 fs. (b) Transient dichroism and the birefringence contributions to the 1-C TG signal for Γ = 100 fs.

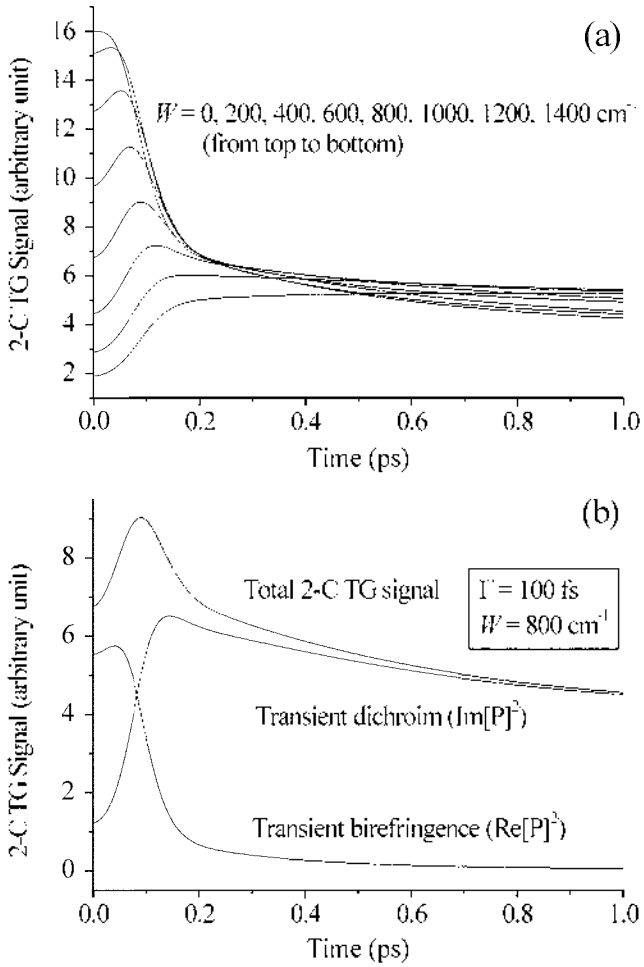

Figure 2. (a) Calculated 'downhill' 2-C TG signals for a detuning W = 0, 200, 400, 600, 800, 1000, 1200, and 1400 cm^{-1}. Here, Γ = 100 fs. (b) Both the transient dichroism and the birefringence contributions to the 2-C TG signal for Γ = 100 fs and W = 800 cm^{-1}.

between the doorway and the window along the solvation energy coordinate.

Since the Stokes shift equals 2λ, when W = 1200 cm^{-1} the window is located at the bottom of the excited state potential energy surface constructed by the chromophore-solvent coupling modes. In this case, the TG signal rises up to a finite value and decays slowly by the excited state population relaxation process. If one carefully examines the 2-C TG signal of W = 1200 cm^{-1} however, the signal reaches a maximum and decays slightly even though the lifetime broadening contribution was not taken into account in the present numerical calculations (see Fig. 2(a)). This is because the homodyne-detected 2-C TG signal contains a contribution from the transient birefringence which initially rise and decays slowly (see the inset of Fig. 1).

Next, the two contributions from the transient birefringence and dichroism are separately plotted in Figure 2(b) in the case when W = 800 cm^{-1} and Γ = 100 fs. Unlike the case of 1-C TG, the transient dichroic but and the transient birefringent contributions are of similar maximum amplitude. In other words, as the detuning increases, the transient birefringence contribution becomes crucial, but the long time decaying pattern is more or less dictated by the transient dichroic response.

As expected, the temporal profile of the 2-C TG signal is strongly dependent on the ultrafast (inertial) decaying component of the solvation correlation function, $S(t)$. Numerically calculated 2-C TG signals are plotted in Figure 3 for a Gaussian decay constant Γ varied from 100 to 500 fs. Here, the detuning factor W is fixed at 800 cm^{-1}. As can be seen in Figure 3, the finite delay time of the signal, which is the time required for the propagating wavepacket to reach the region of the window, increases as the solvation correlation function slows down. Although one can make an attempt to predict this delay time by treating the evolution of the wavepacket as a ballistic motion of which equation of motion is a generalized Langevin equation for a harmonic oscillator (note that the associated time-dependent friction kernel can be obtained by using the Fourier spectrum of the solvation correlation function in Eq. (21)),[15] due to the complication that the homodyne-detected 2-C TG is determined by both the transient dichroism and the transient birefringence contributions it is not straightforward to develop a simple theoretical model for this problem.

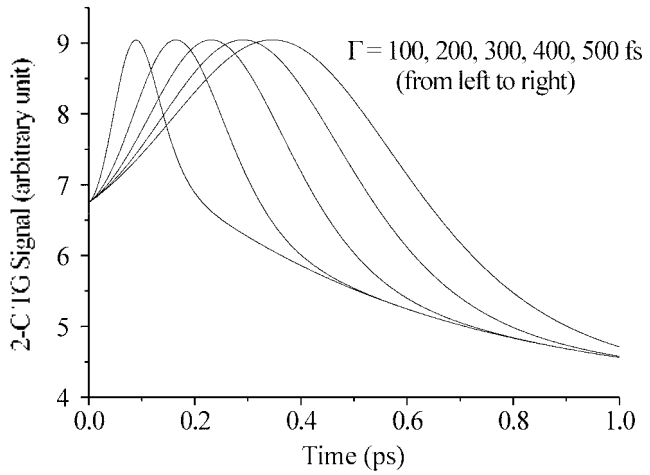

Figure 3. Calculated 2-C TG signals for Γ = 100, 200, 300, 400, and 500 fs. W = 800 cm^{-1}.

Experimental Section

Figure 4 shows the absorption spectra of the dyes IR144 and DTTCI, both dissolved in methanol. Also shown are the spectra of the 800 nm and 750 nm femtosecond pulses used for the experiment. The laser pulses have a duration of 45 fs for all the experiments described. A more detailed description of the pulse generation and experimental set up can be found in reference 16.

Figure 5 shows the four possible homodyne-detected one- and two-color transient grating signals for DTTCI in methanol. Clearly both the uphill and downhill 2C-TG signals differ significantly from the 1C-TG signals and conform to the predictions of Figures 1-3. The two-color signals exhibit rise times of 100-150 fs, while the one-color signals decay monotonically. All the signals contain vibrational wavepacket contributions that were not included in the calculated curves in Figures 1-3. Comparing Figures 2 and 5 suggests that the detuning (833 cm^{-1}) is sufficient to place the window near the bottom of the excited state surface, since no pronounced maximum in the signal is observed.

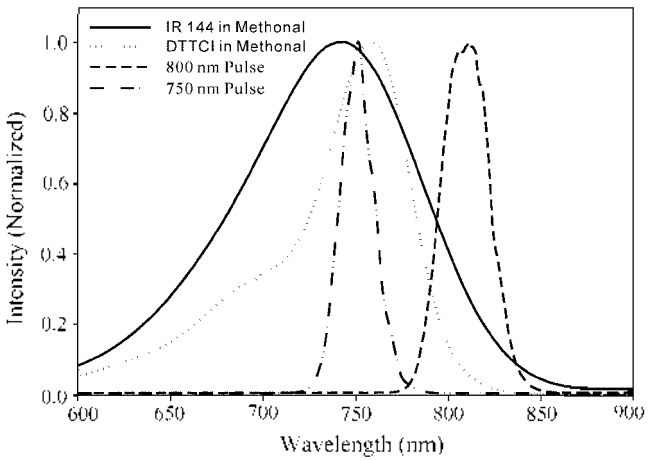

Figure 4. Absorption spectra for IR144 (solid) and DTTCI (dotted) in dilute methanol solution, along with the spectra of the 45 fs 750 nm (dot dashed) and 800 nm (dashed) laser pulses.

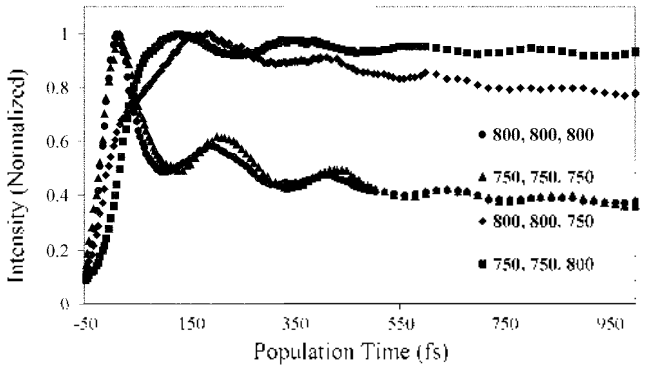

Figure 5. Experimental 1-C TG and 2-C TG signals for DTTCI in methanol. 1-C TG at 800 nm (●) and 750 nm (▲). Both uphill (800, 800, 750 nm, ◆) and downhill (750, 750, 800 nm, ■) results are shown.

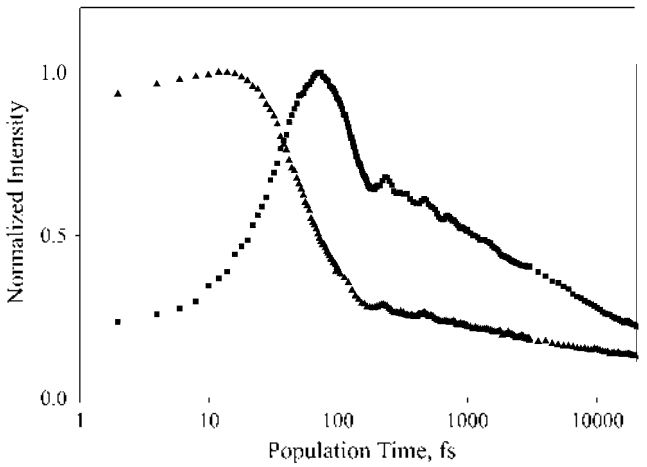

Figure 6. Experimental 1-C TG (750 nm, ▲) and 2-C TG (downhill, 750, 750, 800 nm, ■) signals for IR144 in methanol. Note the logarithmic time axis.

For a system with a larger reorganization energy, a distinct maximum in the 2C-TG signal is expected as the population passes through the window region. IR144 in the same solvent, methanol, has a total Stokes shift of ~1500 cm^{-1} as compared with ~430 cm^{-1} for DTTCI. Figure 6 compares the 1C-TG and 2C-TG for IR144 in MeOH–note the logarithmic timescale. The 2C-TG result corresponds to 750-750-800 nm (downhill) and clearly exhibits a maximum and a rapid decay as expected for intermediate (with respect to 2λ) detunings.

Summary

In the present paper, a theoretical description and experimental illustrations of 2-C TG spectroscopy was presented. When the probe field frequency is different from that of the pump field, the 2-C TG signal exhibits a non-monotonic decaying pattern. Since the frequency of the probe field determines the location of the detection window along the

solvation energy coordinate. the propagating wavepacket achieves maximal overlap only after a finite time delay. which critically depends on the solvation reorganization energy and the time scale of the solvation correlation function. In this regard. the 2-C TG spectroscopy is a useful tool for the investigation of the entire solvation energy surface and correlation time of the chromophore-solvent dynamics. A companion paper in this volume describes two-color photon echo peak shift spectrsocopy.[17]

Acknowledgment. This work was supported by the Creative Research Initiative Program of KISTEP (KOSEF. Korea) to M. Cho. and by a grant from the US National Science Foundation to G. R. Fleming.

References

1. Salcedo, J.; Zorabedian. P.; Hayward, G.; Siegman. A. E.; Fayer. M. D.; Dlott. D. *J. Opt. Soc. Amer.* **1976**, *66*, 1074.
2. Andrews. J. R.; Hochstrasser. R. M. *Chem. Phys. Lett.* **1980**. *76*. 213.
3. Deeg. F. W.; Fayer. M. D. *J. Chem. Phys.* **1989**. *91*. 2269.
4. Goldberg, S. Y.; Bart, E.; Meltsin, A.; Fainberg, B. D.; Huppert, D. *Chem. Phys.* **1994**. *183*. 217.
5. Joo. T.; Jia. Y.; Yu. J.-Y.; Lang. M. J.; Fleming. G. R. *J. Chem. Phys.* **1996**. *104*. 6089.
6. Xu. Q. H.; Ma. Y. Z.; Fleming. G. R. *J. Phys. Chem. A* **2002**. *106*. 10755.
7. Duppen. K.; Weiterkamp. D. P.; Weirsma. D. A. *Chem. Phys. Lett.* **1984**. *108*, 551.
8. Daduse. G.; Ogilvie. J. P.; Schulenburg. P.; Marvet. U.; Miller. R. J. D. *Proc. Natl. Acad. Sci. USA* **2001**. *98*. 6119.
9. Mukamel. S. *Principles of Nonlinear Optical Spectroscopy*. Oxford University Press: New York. 1995.
10. Yan. Y. J.; Mukamel, S. *Phys. Rev. A* **1990**. *41*, 6485.
11. Cho. M.; Yu. J.-Y.; Joo, T.; Nagasawa, Y.; Passino, S. A.; Fleming. G. R. *J. Phys. Chem.* **1996**. *100*. 11944.
12. *Handbook of Mathematical Functions*. Abramowitz. M.; Stegun. I. A.. Eds: Dover Publications INC.: New York. 1972.
13. Cho. M.; Fleming. G. R.; Mukamel. S. *J. Chem. Phys.* **1993**. *98*. 5314.
14. Fleming. G. R.; Cho. M. *Ann. Rev. Phys. Chem.* **1996**, *47*, 103.
15. Cho. M.; Fleming. G. R. *Adv. Chem. Phys.* **1999**. *107*. 311.
16. Agarwal. R.; Prall. B. S.; Rizvi. A. H.; Yang. M.; Fleming. G. R. *J. Chem. Phys.* **2002**. *116*. 6243.
17. Fleming, G. R.; Yang. M.; Agarwal. R.; Prall, B. S.; Kaufman, L. J.; Neuwahl, F. *Bull. Korean Chem. Soc.* **2003**. *24*(8), 1081.